Enantiodivergent epoxidation of alkenes with a photoswitchable phosphate manganese-salen complex

Chen, Xiaofei; Gilissen, Pieter J; Tinnemans, Paul; Vanthuyne, Nicolas; Rutjes, Floris P J T; Feringa, Ben L; Elemans, Johannes A A W; Nolte, Roeland J M

Published in:
Nature synthesis

DOI:
10.1038/s44160-022-00157-7

Publication date:
2022

Published in final edited form as:
Nat Synth. ; 1(11): 873–882. doi:10.1038/s44160-022-00157-7.

Enantiodivergent epoxidation of alkenes with a photoswitchable phosphate manganese-salen complex

Xiaofei Chen[#1], **Pieter J. Gilissen**[#1], **Paul Tinnemans**[1], **Nicolas Vanthuyne**[2], **Floris P. J. T. Rutjes**[1], **Ben L. Feringa**[3], **Johannes A.A.W. Elemans**[1], **Roeland J.M. Nolte**[1]

[1]Institute for Molecules and Materials, Radboud University, Heyendaalseweg 135, 6525 AJ Nijmegen, The Netherlands

[2]Aix Marseille Univ, CNRS, Centrale Marseille, iSm2, Marseille, France

[3]Stratingh Institute for Chemistry, University of Groningen, Nijenborgh 4, 9747 AG Groningen, The Netherlands

[#] These authors contributed equally to this work.

Abstract

The development of enantiodivergent catalysts capable of preparing both enantiomeric products from one substrate in a controlled fashion is challenging. Introducing a switching function into the catalyst can address this challenge, allowing the chiral reaction environment to reversibly change during catalysis. Here we report a photoswitchable phosphate ligand, derived from 2,2'-biphenol, which axially coordinates as the counter ion to an achiral manganese(III) salen catalyst, providing the latter with the ability to switch stereoselectivity in the epoxidation of alkenes. The enantiomers of the chiral ligand exist as a pair of pseudo-enantiomers, which can be interconverted by irradiation with light of different wavelengths. The opposite axial chirality of these pseudo-enantiomers is efficiently transferred to the manganese(III) salen catalyst. With this switchable supramolecular catalyst, the enantioselectivity of the epoxidation of a variety of alkenes can be controlled, resulting in opposite enantiomeric excesses of the epoxide products. This transfer of chirality from a photoswitchable anionic ligand to a metal complex broadens the scope of supramolecular catalysts.

Correspondence to: Ben L. Feringa; Johannes A.A.W. Elemans; Roeland J.M. Nolte.

r.nolte@science.ru.nl; j.elemans@science.ru.nl; b.l.feringa@rug.nl.

Author contributions. R.J.M.N. conceived the project. P.J.G. and F.P.J.T.R. designed the synthesis of compound **1**. P.J.G. carried out the synthesis of **1** and investigated the photochemical properties of compounds **1** and **Mn2**. X.C. performed the catalysis experiments and grew the crystals. P.T. determined and analysed the crystal structure. N.V. separated the enantiomers of **1** by chiral HPLC. B.L.F contributed with his knowledge on molecular photoswitches. R.J.M.N. and J.A.A.W.E. supervised the project. All authors discussed the results, and helped write and discuss the manuscript.

Competing Interests. The authors declare no competing interests.

Europe PMC Funders Author Manuscripts

Introduction

Chirality is ubiquitous amongst molecules in nature, such as amino acids, sugars, proteins, and DNA.[1] In cells, enzymes precisely control life processes by carrying out strictly enantioselective catalytic transformations on bound substrates.[2] Taking the stereochemical fidelity of such processes as a blueprint, great advances have been made in stereoselective syntheses in academic laboratories and pharmaceutical industries. Although many chiral catalysts capable of producing close to enantiomerically pure products have been developed, the design of enantiodivergent catalysts, which are capable of producing both enantiomeric products of a reaction via a switching function, is still an intriguing challenge.[3–6] To achieve controllable switching, a specific design of molecules that can exist in various distinct conformations is required. In 1999, the first example of a molecular motor displaying light- and heat-controlled unidirectional rotating behaviour, was reported.[7] This molecular motor relies on the *cis-trans* isomerization of an overcrowded alkene located between an aromatic stator and rotor fragment, which is accompanied by a change in the relative helicity of the fragments, adopting either an *M* or a *P* configuration. The use of light as a non-invasive external stimulus for the isomerization reaction excludes the undesired generation of chemical waste or the occurrence of side reactions.[8] The first-generation molecular motors[7] required both photochemical and thermal isomerization steps to interconvert the pseudo-enantiomers. In contrast, the later developed second-generation molecular motors are equipped with a symmetric fluorenyl stator and can be interconverted by solely utilizing light (Fig. 1a).[9,10] Recent advances in constructing asymmetric organocatalysts with an implemented “on-off” function have drawn attention because they are capable of performing complicated tasks when they are triggered by external stimuli, such as light, changes in solvent or pH, or the binding of metals.[3,11–13] However, the development of enantiodivergent catalysts is still highly challenging, and only few examples of such systems have been reported. A first-generation molecular motor equipped with organocatalytic functions has been applied as a catalyst in an asymmetric Michael addition reaction, producing a mixture of adducts with 50% e.e., while after a thermally activated reversal in helicity of the motor, the adduct with an opposite enantioselectivity of 54% e.e. was preferentially obtained (Δe.e. = 104%).[14] First-generation molecular motors have also been used as a stereodivergent catalyst in Henry reactions (Δe.e. = up to 116%),[15] as a ligand in a palladium-catalyzed desymmetrization reaction (Δe.e. = 174%),[16] and as anion binding catalysts (Δe.e. = up to 142%).[17] A second-generation molecular motor has been used as a photoswitchable catalyst for the enantiodivergent addition of diethylzinc to aldehydes (Δe.e. = up to 113%).[10] Recently, Leigh et al. reported a switchable molecular shuttle, which could stereoselectively catalyze the conjugate addition of aldehydes to vinyl sulfones, yielding products with opposite enantiomeric configurations (Δe.e. = up to 60%).[18]

Chiral phosphates as ligands or counter ions in ion-paired catalysts can be of importance in enantioselective catalysis, because they can strongly render and amplify chirality during the catalytic reaction at the metal center[19,20] (for a discussion of ion-paired catalysis and related concepts see reference 19). In 2002, Lacour et al. reported pioneering work in which chiral hexacoordinated phosphate anions improved the enantioselectivity of an oxone-mediated epoxidation.[21] More recently, chiral phosphates were employed in asymmetric

Brønsted acid-based catalysis,[22] and gold,[23] palladium[24] and iridium-based[25] transition metal catalysis. A typical example of such a chiral phosphate is the 3,3'-bisaryl-substituted BINOL-derivative shown in Fig. 1b, which can provide enantioselectivity in catalytic reactions.[26] List et al. reported a series of ion-paired catalysts in which chiral BINOL-based phosphate counter ions coordinated to a manganese(III) salen complex displayed excellent enantioselectivities (up to 96% e.e.) in the epoxidation of alkenes.[27,28]

Current work in our group aims at encoding binary information into polymer chains, by threading them through a cavity-containing catalyst that can write chiral epoxides, where (*R*,*R*)-epoxide = digit 1, (*S*,*S*)-epoxide = digit 0.[29] In order to make this writing stereo-controllable, we set out to investigate enantiodivergent epoxidation catalysts that can be switched non-invasively with light. Herein, we report manganese(III) salen phosphate complex **Mn2**, which consists of two components: an achiral manganese(III) salen complex (Fig.1c), which is capable of catalytically transferring an oxygen atom from an oxidant to an olefin substrate to generate an epoxide, and a photoresponsive 2,2'-biphenol-derived phosphate ligand **1** (Fig. 1d), which coordinates to the manganese(III) center via one of the oxygen atoms attached to the prochiral phosphorus center, thereby inducing chirality into the salen complex. Upon irradiation with light, the overcrowded alkene moiety of this counter ion switches helicity (*M* to *P*), thereby selectively switching the axial chirality of the 2,2'-biphenol moiety (R_a to S_a), which in turn should switch the chiral environment of the manganese(III) salen (Fig. 1e). As a result, the catalyst becomes capable of carrying out enantiodivergent epoxidation reactions controlled by the photoswitchable anionic ligand.

Results and discussion

Design

The design of the photoswitchable molecular catalyst is inspired by the previously reported light-responsive motors derived from 2,2'-biphenol (Fig. 1a).[10,30] The aromatic fragments connected to the overcrowded alkene are synthesized separately, which allows for their separate modification. The biphenol-based moiety contains a stereogenic center with a methyl substituent, which controls the unidirectionality of the rotation of the motor.[31] Second-generation molecular motors composed of a symmetric fluorenyl stator and a six-membered ring rotor have been reported as excellent chiroptical switches, because of their high photostationary state (PSS) ratios, as well as for the thermal stability of their metastable isomer ($t_{1/2}$ ~ years).[32] In the case that the initial stereoisomer and the stereoisomer obtained by photochemical isomerization are both relatively stable, it becomes possible to use the motor as a two-state molecular switch, and by irradiation with light of two different wavelengths, the *M* and *P* helical configurations of the motor can be reversibly switched. These stable helicities may continuously transfer and amplify the chirality of a metal complex during catalytic reactions.[10,30]

The use of chiral manganese(III) salen derivatives as catalysts for the asymmetric epoxidation of alkenes has been extensively described by the groups of Jacobsen[33] and Katsuki.[34] Although a manganese(III) salen containing an ethylene-bridge is symmetric (Fig 1c), and cannot be used as an asymmetric catalyst itself, the axial coordination of a chiral counter ion to the metal center can induce a chiral configuration, leading to high

enantioselectivities in oxidation reactions.[27,28,35] Simultaneously, such a coordination can lead to an increase in reactivity of the catalyst.[36] We envisaged that, after deprotonation, the phosphoric acid-functionalized molecular switch **1** can act as an anionic chiral inducer ligand for a manganese(III) salen epoxidation catalyst, providing the resulting ion-paired complex **Mn2** with inherent switchable chirality for the enantiodivergent epoxidation of alkenes.

Specifically, **Mn2** includes five chiral elements (Fig. 1e): (1) the point chirality at the stereogenic center with the methyl substituent attached (magenta); (2) the helicity of the aromatic fragments connected to the overcrowded alkene (blue); (3) the bis-aryl axial chirality (S_a or R_a); (4) the dynamic helical geometry between the aromatic rings of the salen and switch (*P* or *M)* (black); (5) the chirality of the phosphorus atom after coordination of the phosphate group to the manganese(III) salen.

We reasoned that, upon its coordination to the manganese(III) center, a pure enantiomer of (deprotonated) **1** can transfer its helicity to the salen backbone and induce a specifically twisted conformation of the ethylene linker, thereby enabling **Mn2** to enantioselectively epoxidize an alkene. Upon irradiation of the catalyst with light with a wavelength at which the overcrowded alkene absorbs (the $\pi \rightarrow \pi^*$ transition), the phosphate ligand is expected to be converted to its pseudo-enantiomer, thereby transferring its opposite helicity to the salen and providing the ethylene-bridge with an opposite twist. The catalyst is then expected to preferably catalyze the formation of the opposite enantiomer of the epoxide. In other words, the helicity of the chiral anionic phosphate ligand can be modulated with light, which, as a consequence, is directing the enantioselectivity of the Mn-salen catalyst towards either enantiomer of the chiral epoxide product externally and on demand.

Synthesis

The synthesis and resolution of ion-paired catalyst **Mn2** is depicted in Fig. 2. The synthesis of the motor-containing phosphoric acid **1** started from commercially available 4-arylbutanoic acid **3**, which was dibrominated with bromine at the *ortho-positions* with respect to the methoxy-substituent. An intramolecular Friedel–Crafts acylation of the crude dibromocarboxylic acid was accomplished with Eaton's reagent at mildly elevated temperature. The key synthetic step was the regioselective introduction of the *tert*-butylphenyl substituent onto aryl dibromide **4**. The combination of Pd_2dba_3 as palladium source combined with the bulky bidentate phosphine ligand bis[(2-diphenylphosphino)phenyl] ether (DPEPhos) allowed us to obtain cross-coupled product **5** in good yield. 2-Bromoanisole **6** was cross-coupled under standard Suzuki–Miyaura conditions to afford the biphenyl derivative **7**. *ortho*-Lithiation of compound **7** followed by a reaction of the aryl lithium species with trimethylborate and aqueous workup yielded boronic acid **8**. A subsequent Suzuki–Miyaura reaction between bromide **5** and boronic acid **8** afforded cross-coupled compound **9** in very good yield. The stereogenic center was introduced by α-methylation, furnishing ketone **10** in excellent yield. The reaction of ketone **10** with hydrazine monohydrate in *n*-butanol using scandium(III) triflate as the catalyst afforded hydrazone **11**. The latter compound was oxidized *in situ* using [bis(trifluoroacetoxy)iodo]benzene (PIFA), and the resulting diazo intermediate was reacted

with freshly prepared thioketone **12**.[37] The Barton–Kellogg olefination initially afforded an episulfide intermediate, which was desulfurized by tris(dimethylamino)phosphine (HMPT), providing overcrowded alkene **13** in reasonable yield after this three-step sequence. Next, the methyl protecting groups were removed with methylmagnesium iodide,[10] affording diol **14** in nearly quantitative yield. Compounds **10**, **11**, **13**, and **14** were all obtained as racemic mixtures, of which each enantiomer was composed of two axially chiral conformers due to the non-fixed axial chirality. The biaryl axis was fixed in a specific axial chirality once diol **14** was reacted with phosphoryl chloride, with the resulting seven-membered phosphate ring blocking the diol in the *syn*-conformation, resulting in the enantiomers (*S,M,R*$_a$)-**1** and (*R,P,S*$_a$)-**1**. In these enantiomers, the helical and axial chirality are dictated by the configuration of the stereogenic carbon center. Previous investigations on aryl substituted molecular motors and switches have shown that the aryl substituent in the rotor part is always parallel to the fluorenyl lower half.[10,30,38] The enantiomers of phosphoric acid **1** were resolved by preparative chiral high-performance liquid chromatography (HPLC) (Supplementary Fig. 1-4). Their absolute configurations were determined by the comparison of their electronic circular dichroism (Supplementary Fig. 4) spectra to those of the diol rotor reported in 2018 (Fig. 1a).[10] The first and second eluted enantiomers of phosphoric acid **1** displayed positive and negative Cotton effects for the $\pi \rightarrow \pi^*$ transition (λ = 356 nm), corresponding to molecular motors with (*M*)- and (*P*)-helicity, respectively. The relative (*R,P,S*$_a$)- and (*S,M,R*$_a$)-stereochemistry of **1** was deduced from 2D Nuclear Overhauser Effect Spectroscopy (NOESY) experiments. Finally, the reaction of enantiopure or racemic phosphoric acid **1** with manganese(III) salen derivative **Mn15**[39] afforded the enantiopure or the racemic manganese(III) salen phosphate complexes **Mn2**, respectively.

Photochemical isomerization

We first investigated the switching properties of the enantiopure phosphoric acid ligand isomer (*S,M,R*$_a$)-**1** and the corresponding ion-paired complex (*S,M,R*$_a$)-**Mn2** (Fig. 3.) The $\pi \rightarrow \pi^*$ transition of (*S,M,R*$_a$)-**1** was determined to be at λ_{max} = 356 nm (Fig. 3c). Hence, we could accomplish the photochemical isomerization of stable (*S,M,R*$_a$)-**1** to metastable (*S,P,S*$_a$)-**1** with a light-emitting diode (LED) emitting UV-light at λ_{max} = 365 nm (Fig. 3c). The isomerization was accompanied by a bathochromic shift ($\Delta\lambda$ = 43 nm) of the main absorption band at 356 nm, which is indicative of an increase in strain in the original alkene double bond after irradiation.[32] The presence of an isosbestic point at λ = 379 nm indicates a clean unimolecular process. The Cotton effect associated with the main absorption band (positive circular dichroism (CD) signal at λ = 356 nm) was inverted (negative CD signal at λ = 399 nm), indicating an inversion of helicity, and an inversion of the CD sign at λ = 300 nm was observed. When the resulting PSS$_{365}$-mixture containing metastable (*S,P,S*$_a$)-**1** was irradiated with visible light at λ = 470 nm, the opposite spectral changes were observed while the isosbestic point at λ = 379 nm was retained (Fig. 3d). To investigate the reversibility and stability of the switch, we subjected the solution of (*S,M,R*$_a$)-**1** to a series of isomerization cycles (Fig. 3e), and monitored the absorption maxima of the stable isomer (*S,M,R*$_a$)-**1** (λ = 356 nm), the metastable isomer (*S,P,S*$_a$)-**1** (λ = 399 nm), and the CD signal at λ = 300 nm. All these maxima showed no signs of switching fatigue after five cycles.

The switching processes of **1** were investigated in more detail with the help of NMR spectroscopy (Fig. 4). To this end, we irradiated a solution of stable *Rac*-**1** (Fig. 4b stable) *in situ* with UV-light of λ = 365 nm for 45 min at 20 °C. A new set of signals appeared in the NMR spectrum, corresponding to the metastable isomer of *Rac*-**1** (Fig. 4b PSS $_{365}$). Comparison of the integrals of the ^{1}H NMR spectroscopy resonances of the stable and metastable isomers allowed the determination of the photostationary state: PSS_{365} metastable:stable ≈ 95:5. This PSS-ratio is higher than that of similar second-generation molecular motors.[10,30] Noticeably, the NMR spectrum of metastable *Rac*-**1** recorded after the solution had been stored under ambient conditions for two weeks was nearly identical to the spectrum that was recorded directly after the irradiation process (Fig. 4b PSS $_{365}$ after 2 weeks), illustrating that the metastable state possesses a high thermal stability as well as an insensitivity to ambient light. When the sample was subsequently irradiated with visible light (λ = 470 nm) at 20 °C for 18 h, the stable state was regenerated nearly quantitatively: PSS_{470} metastable:stable ≈ 5:95 (Fig. 4b PSS $_{470}$).

In a next series of experiments, we investigated the photoisomerization processes of ion-paired catalyst **Mn2** with UV-vis and CD spectroscopy (Fig. 3b). The use of ^{1}H NMR spectroscopy was not possible due to the paramagnetic nature of the compound. The changes in the UV-vis spectra of **Mn2** upon photochemical isomerization with UV-light at λ = 365 nm (Fig. 3f, top) were reminiscent of those observed for phosphoric acid **1**, specifically a bathochromic shift of the absorption maximum of the overcrowded alkene moiety, and a clear isosbestic point at λ = 381 nm. The CD spectrum of (*S,M,R*$_a$)-**Mn2** revealed that the chiral information in the phosphate ligand is effectively transferred to the manganese salen moiety, which is evidenced by the CD absorption at λ = 430 nm (Fig. 3f, bottom). Upon photochemical isomerization, the CD sign of **Mn2** at λ = 300 nm changed sign from positive to negative, akin to what was observed for phosphoric acid **1**. More importantly, the inversion of the CD sign at λ = 430 nm indicated that the chirality of the manganese(III) salen moiety could be effectively tuned by the switchable phosphate ligand. The reverse photochemical isomerization of the metastable ion pair (*S,P,S*$_a$)-**Mn2** (PSS_{365}) to the stable ion pair (*S,M,R*$_a$)-**Mn2** was accomplished by irradiation with visible light at λ = 470 nm (Fig. 3g). The isomerization processes of **Mn2** were reversible for at least five cycles (Fig. 3h), which agrees with the behavior that was observed for phosphoric acid **1**. Although quantitative information about the PSS-ratios could not be obtained from the above spectroscopic investigations, we reason that the PSS_{365} and PSS_{470}-ratios of **1** and **Mn2** are very similar, since their differences in absorbance at λ = 356 (ΔAbs ≈ 0.2) and 399 nm (ΔAbs ≈ 0.2) and CD intensity at λ = 300 nm (ΔCD ≈ 35 mdeg) between the stable and metastable states are nearly identical under the same conditions.

X-ray crystallography

Besides obtaining spectroscopic evidence for the photochemical isomerization processes of **Mn2**, we also investigated these by determining the crystal structures of **Mn2** in the stable and metastable states. Initially, we tried to obtain single crystals of the enantiopure catalysts (*S,M,R*$_a$)-**Mn2** and (*R,P,S*$_a$)-**Mn2**, but unfortunately we were unsuccessful. However, a single crystal of stable *Rac*-**Mn2** could be obtained by the slow evaporation of a solution of the complex in toluene/*n*-heptane (1:8, v/v). From this crystal the X-ray structure of

the complex could be determined (Supplementary Fig. 5). The unit cell of the crystal contains both enantiomers of the complex, (*S,M,R*$_a$)-**Mn2** and (*R,P,S*a)-**Mn2**. They display opposite helicities and axial chiralities of the overcrowded alkene axis and the biaryl moiety, respectively. In addition, they possess opposite fixed point chirality at the stereogenic center to which the methyl substituent is attached. The distance between the manganese atom and the phosphate oxygen atom is 2.04 Å, which indicates that the phosphate acts as an anionic ligand, which is strongly attached to the manganese center. Consequently, it may be expected that the chirality of the switch connected to the phosphate will be transferred to the manganese(III) salen, providing it with the ability to carry out asymmetric catalysis. Irradiation of a solution of stable *Rac*-**Mn2** (concentration = 1 mg/mL in CH_2Cl_2) for 30 minutes with λ = 365 nm light furnished a solution of metastable *Rac*-**Mn2**. Evaporation of the solvent followed by crystallization from toluene/*n*-heptane (1:8, v/v) furnished metastable *Rac*-**Mn2** in the crystalline state. In Fig. 5 the X-ray crystal structures of stable (*S,M,R*$_a$)-**Mn2** (Fig. 5a left) and metastable (*S,P,S*$_a$)-**Mn2** (Fig. 5a right) are compared. The comparison reveals that after light irradiation not only the helicity of the overcrowded alkene (blue color) changes (*M* to *P*), but also the axial chirality (*R*$_a$ to *S*$_a$), the twist in the ethylene bridge (magenta color) of the salen ligand (*M* to *P*), and the central chirality of the stereogenic phosphorus center (*S* to *R*). The change in configuration of the stereogenic phosphorus center reveals that during the irradiation or crystallization process, the phosphate anionic ligand has to dissociate from the manganese(III) center and later re-associate via the other oxygen atom. Although these solid state structures are considered to be pseudo-enantiomers, their behavior in solution might be different, for example, the phosphate ligand may be bound via either of the two oxygen atoms, creating different diastereomeric complexes. Nonetheless, the above-mentioned chirality changes are thought to lie at the origin of the observed photoswitchable enantioselective epoxidation catalysis (vide infra).

Switchable asymmetric catalysis

Having established the light-switching properties of **Mn2** by spectroscopic and X-ray crystallographic techniques, we employed the catalyst in the switchable epoxidation of alkenes. Using the chromene derivative **17a** as a model substrate, iodosyl benzene as the oxygen donor, and (*S,M,R*$_a$)-**Mn2** as the catalyst in dry benzene, the alkene was converted nearly quantitatively and the enantiomers of the epoxide product were isolated in a combined yield of 89%. Analysis of the mixture by chiral HPLC revealed that the two epoxide enantiomers were formed in a ratio of 13:87 (major enantiomer: (1a*R*,7b*R*)-**17b**, e.e. = 74%) (Table 1, entry 1 and Fig. 6b upper). In a separate experiment, we first irradiated the stable catalyst (*S,M,R*$_a$)-**Mn2** with light (λ = 365 nm for 30 min, concentration = 1 mg/mL in CH_2Cl_2) to generate metastable catalyst (*S,P,S*$_a$)-**Mn2** after removal of the solvent. Using this catalyst in the epoxidation of **17a** gave a combined epoxide yield of 73%, but now in an opposite enantiomeric ratio of 71:29 (major enantiomer: (1a*S*,7b*S*)-**17b**, e.e. = 42%) as revealed by chiral HPLC (Table 1, entry 2 and Fig. 6b lower). These experiments confirm that the phosphate ligand is indeed capable of efficiently transferring its chirality to the manganese(III) salen, and that light-induced switching of the helicity of the ligand leads to switching of the enantioselectivity of the catalyst.

We found that catalytic reactions in freshly dried and distilled benzene and the use of 2.5 mol% of **Mn2** catalyst with respect to the substrate gave the most optimal results (Supplementary Table 2). The presence of water in the benzene solution turned out to have a negative impact on catalyst performance, both in terms of yield and stereoselectivity (Supplementary Table 3). We attribute this decrease in performance to a weakening of the coordination bond between the manganese center and the phosphate ligand, resulting in a decrease in activation of the metal center as well as a decrease in chirality transfer from the ligand to the salen backbone. A further decrease in solvent polarity by the addition of up to 50% (v/v) of *n*-heptane to the benzene solution did not improve the conversion nor the extent of enantioselectivity (Supplementary Table 4), neither did variations in reaction temperature (Supplementary Table 5).

We then confirmed the absolute configurations of catalysts **Mn2** by using the chiral Jacobsen manganese(III) salen complexes (*M,R,R*)-**Mn16** and (*P,S,S*)-**Mn16** as reference catalysts for the epoxidation of alkene **17a** (Fig. 6).[40] When (*M,R,R*)-**Mn16** was used as the catalyst, the trend in enantioselectivity of the epoxidation was the same as that observed when (S,M,R_a)-**Mn2** was used (Fig. 6a upper and 6b upper). Catalysts (*P,S,S*)-**Mn16** and (S,P,S_a)-**Mn2** showed the reverse trend (Figs. 6a lower and 6b lower), as expected. The key origin for the formation of a preferred chiral configuration of the epoxide is the specific induced chirality present in the salen ligand. The fact that (*M,R,R*)-**Mn16** and (S,M,R_a)-**Mn2** display the same trend in enantioselectivity indicates that they share a similar (*M*)-twist in their ligand backbone, while (*P,S,S*)-**Mn16** and (S,P,S_a)-**Mn2** share a (*P*)-twist. Based on the crystal structure of *Rac*-**Mn2** (Fig. 3), we thus can assign the first eluted fraction from the chiral HPLC to (S,M,R_a)-**1** and the second to (R,P,S_a)-**1** (Fig. 2), which is in line with the results obtained from the CD measurements.

To investigate the scope of the reactions catalyzed by **Mn2**, we investigated the enantiodivergent epoxidation with different types of alkenes (Table 1). All reactions were performed in duplicate showing reproducibility of the catalytic system. Chromene derivatives with various substituents (for example, NO_2, CN, Ph, OAc) were smoothly converted into their corresponding epoxides, and so were various internally conjugated and terminal olefins. In all cases, light-induced switching of the catalyst resulted in opposite enantioselectivities of the epoxidation. For substrate **17a**, we also investigated the catalytic performance of the other enantiomer, (R,P,S_a)-**Mn2**. This catalyst (Table 1, entry 3) and its irradiated metastable isomer (R,M,R_a)-**Mn2** (Table 1, entry 4) gave epoxide product **17b** in opposite stereoselectivities as compared to (S,M,R_a)-**Mn2** and (S,P,S_a)-**Mn2**, respectively. The absolute configurations of the enantioenriched epoxide products could be correlated to the coupled helical and axial chirality of the anionic phosphate ligand of the **Mn2** catalyst. The **Mn2** catalysts with the (M,R_a)-configuration, stable (S,M,R_a)-**Mn2** and metastable (R,M,R_a)-**Mn2**, preferentially produced epoxides with the (*R*)-configuration on the carbon adjacent to the aromatic ring, while the opposite selectivity was found for the stable (R,P,S_a)-**Mn2** and metastable (S,P,S_a)-**Mn2** catalysts. The only exception to this trend was the trisubstituted olefin 1-phenylcyclohexene **24a**, which showed opposite, albeit low enantioselectivity (Table 1, entries 17 and 18).

The enantioselective performance of the isomers of the **Mn2** catalyst can be expressed in terms of the difference in e.e. value (maximum obtainable Δe.e. = 200%). Epoxide **17b** was produced with the highest Δe.e. (up to 118%). An alternative measure of performance might be the enantio-divergence (e.d.) of the epoxidation, which we define as the ratio of the enantiomeric excess values of the enantioenriched epoxides when produced by metastable-**Mn2** versus stable-**Mn2** (maximum obtainable e.d. = 100%). While the absolute enantioenrichment of the styrene oxides **21b**–**23b** is rather low (e.e. < 25%), the enantio-divergence is significant (50–100%). In all cases, catalysts **Mn2** in their stable states produced epoxides with higher enantiomeric excesses than their metastable isomers that were obtained after irradiation with light of λ = 365 nm. We attribute this difference to two factors. Firstly, the photochemical isomerization is not complete, the PSS_{365}-ratio metastable:stable isomer is not 100:0. Secondly, the phosphorus atom of the phosphate moiety becomes intrinsically chiral once one of its oxygen atoms coordinates to the manganese center. If the oxygen-manganese bond remains intact during the isomerization process, in other words the phosphorus atom retains its chirality, the stable and metastable complexes no longer are pseudo-enantiomers, but rather behave as diastereomers and a difference in e.e. is expected. In order to investigate the role of the stereogenic phosphorus center and the role of the PSS ratio of **Mn2**, we also prepared all isomers of catalyst **Mn2** in different complexation-irradiation orders (Supplementary Fig. 9 and 10). For instance, metastable catalyst (*S*,*P*,S_a)-**Mn2** could be prepared by the irradiation of stable (*S*,*M*,R_a)-**Mn2**, as described above, but it could also be prepared by the irradiation of stable (*S*,*M*,R_a)-**1** followed by complexation of metastable (*S*,*P*,S_a)-**1** to the achiral manganese(III) salen **Mn15**. The resulting catalyst, obtained via the irradiation-complexation sequence, performed equally well in terms of enantioselectivity (46% e.e. vs 42–44% e.e.) as the same catalyst obtained via the complexation-irradiation sequence (for details of all other isomers see Supplementary Figs. 9 and 10). This result implies that the PSS_{365} ratio of catalyst **Mn2** is very similar to that of ligand **1** itself (95:5), as is also suggested by the similarities observed in the UV-vis and CD measurements. In addition, we can conclude that in solution the catalysts stable (*S*,*M*,R_a)-**Mn2** and metastable (*S*,*P*,S_a)-**Mn2** act as diastereomers rather than pseudo-enantiomers. An alternative explanation for the lower enantioselectivity of the metastable catalysts with respect to the stable catalysts might be that in solution the diastereomeric catalysts with the (*R*)- and (*S*)-phosphorus configuration are in equilibrium, with the equilibrium constant being different between the stable and metastable isomers of the anionic phosphate ligand. In contrast, the X-ray structures shown in Fig. 5 and in the Supplementary Figs. 5,6 and Supplementary Table 6 indicate that the stable and the metastable complexes are pseudo-enantiomers, meaning that the manganese-oxygen bond becomes broken during the photoisomerization process and that the phosphorus center inverts its absolute stereochemistry. It should be noted that this reasoning is based on the solid-state X-ray structures and that the described situation may be different for the structures in solution. Further research on the structural properties of these supramolecular catalysts and the impact on the mechanism and enantioselectivity of the catalytic reactions are currently ongoing.

Europe PMC Funders Author Manuscripts

Conclusion

A supramolecular catalyst consisting of a photoresponsive phosphate anionic ligand coordinated to a manganese(III) salen has been developed and shown to exhibit significant levels of enantioselectivity in the epoxidation of alkenes. Irradiation of the biphenol-derived molecular motor connected to the phosphate changes its helicity, which in turn results in an inversion in axial chirality. Transfer of the axial chirality from the phosphate ligand to the salen backbone governed significant degrees of stereoselectivity during catalysis. The stable and metastable isomers of catalyst **Mn2** were able to furnish epoxides with various degrees of enantio-divergence (up to 100%). The epoxidation of a variety of alkenes revealed that internal alkenes are more prone to enantioselective epoxidation than terminal ones, with Δe.e. values of up to 118%. Although the current catalytic system displays significant degrees of enantio-divergence, it requires optimization in the sense of irradiation time-response before it can be considered a truly dynamic system. Nevertheless, we envision that the use of switchable photoresponsive anionic ligands as chirality inducers, as shown here, may be widely applicable in transition metal catalysis and may significantly broaden the chiral pool for the development of more complex and efficient catalytic systems.

Methods

General procedure for the catalytic epoxidation reactions. A pre-dried Schlenk finger was charged with racemic or enantiopure catalyst **Mn2** (3.2 mg, 2.5 mol%). The Schlenk finger was evacuated and backfilled with argon (3 times). Then, alkene substrate (0.10 mmol, 1.0 equiv.) and dry benzene (1.9 mL) were added and the resulting brown solution was stirred at 20 °C for 5 minutes. Subsequently, iodosylbenzene (26.4 mg, 0.12 mmol, 1.2 equiv.) was added in one portion. The resulting mixture was stirred for 16 hours in the dark under an argon atmosphere. Thereafter, the solvent was removed in vacuo and the crude product was purified by preparative thin-layer chromatography (TLC) to afford the isolated epoxide product. Enantiomeric excess values were determined by chiral HPLC analysis.

Supplementary Material

Refer to Web version on PubMed Central for supplementary material.

Acknowledgements

This work was financially supported by the European Research Council (ERC Advanced Grant No. 74092 to R. J. M. N. and ERC Advanced Grant No. 227897 to B.L.F.) and by the Dutch Ministry of Education, Culture, and Science (Gravitation program 024.001.035).

Data Availability

The authors declare that the data supporting the findings of this study are included in the paper and the Supplementary Information file. Any further relevant data are available from the corresponding authors on request. Crystallographic data for the structure *Rac*-**Mn2** reported in this article has been deposited at the Cambridge Crystallographic Data Centre (CCDC), under deposition number 2125340. Copies of the data can be obtained free of charge via https://www.ccdc.cam.ac.uk/structures/.

References

1. Bonner WA. Chirality and life. Origins Life Evol Biosphere. 1995; 25: 175–190.
2. Brady D, Jordaan J. Advances in enzyme immobilisation. Biotechnol Lett. 2009; 31: 1639. [PubMed: 19590826]
3. Vlatković M, Collins BS, Feringa BL. Dynamic responsive systems for catalytic function. Chem Eur J. 2016; 22: 17080–17111. [PubMed: 27717167]
4. Dorel R, Feringa BL. Photoswitchable catalysis based on the isomerisation of double bonds. Chem Commun. 2019; 55: 6477–6486.
5. Göstl R, Senf A, Hecht S. Remote-controlling chemical reactions by light: Towards chemistry with high spatio-temporal resolution. Chem Soc Rev. 2014; 43: 1982–1996. [PubMed: 24413363]
6. Blanco V, Leigh DA, Marcos V. Artificial switchable catalysts. Chem Soc Rev. 2015; 44: 5341–5370. [PubMed: 25962337]
7. Koumura N, Zijlstra RW, Van Delden RA, Harada N, Feringa BL. Light-driven monodirectional molecular rotor. Nature. 1999; 401: 152–155. [PubMed: 10490022]
8. García-López V, Liu D, Tour JM. Light-activated organic molecular motors and their applications. Chem Rev. 2020; 120: 79–124. [PubMed: 31849216]
9. Koumura N, Geertsema EM, Van Gelder MB, Meetsma A, Feringa BL. Second generation light-driven molecular motors. Unidirectional rotation controlled by a single stereogenic center with near-perfect photoequilibria and acceleration of the speed of rotation by structural modification. J Am Chem Soc. 2002; 124: 5037–5051. [PubMed: 11982368]
10. Pizzolato SF, et al. Central-to-helical-to-axial-to-central transfer of chirality with a photoresponsive catalyst. J Am Chem Soc. 2018; 140: 17278–17289. [PubMed: 30458108]
11. Van Dijk L, et al. Molecular machines for catalysis. Nat Rev Chem. 2018; 2 0117
12. Ihrig SP, Eisenreich F, Hecht S. Photoswitchable polymerization catalysis: state of the art, challenges, and perspectives. Chem Commun. 2019; 55: 4290–4298.
13. Romanazzi G, Degennaro L, Mastrorilli P, Luisi R. Chiral switchable catalysts for dynamic control of enantioselectivity. ACS Catal. 2017; 7: 4100–4114.
14. Wang J, Feringa BL. Dynamic control of chiral space in a catalytic asymmetric reaction using a molecular motor. Science. 2011; 331: 1429–1432. [PubMed: 21310964]
15. Vlatković M, Bernardi L, Otten E, Feringa BL. Dual stereocontrol over the Henry reaction using a light-and heat-triggered organocatalyst. Chem Commun. 2014; 50: 7773–7775.
16. Zhao D, Neubauer TM, Feringa BL. Dynamic control of chirality in phosphine ligands for enantioselective catalysis. Nat Commun. 2015; 6: 6652. [PubMed: 25806856]
17. Dorel R, Feringa BL. Stereodivergent anion binding catalysis with molecular motors. Angew Chem Int Ed. 2020; 59: 785–789.
18. Dommaschk M, Echavarren J, Leigh DA, Marcos V, Singleton TA. Dynamic control of chiral space through local symmetry breaking in a rotaxane organocatalyst. Angew Chem Int Ed. 2019; 58: 14955–14958.
19. Brak K, Jacobsen EN. Asymmetric ion-pairing catalysis. Angew Chem Int Ed. 2013; 52: 534–561.
20. Phipps RJ, Hamilton GL, Toste FD. The progression of chiral anions from concepts to applications in asymmetric catalysis. Nat Chem. 2012; 4: 603–614. [PubMed: 22824891]
21. Lacour J, Monchaud D, Marsol C. Effect of the medium on the oxaziridinium-catalyzed enantioselective epoxidation. Tetrahedron Lett. 2002; 43: 8257–8260.
22. Čorić I, List B. Asymmetric spiroacetalization catalysed by confined Brønsted acids. Nature. 2012; 483: 315–319. [PubMed: 22422266]
23. LaLonde R, Wang Z, Mba M, Lackner A, Toste FD. Gold (I)-catalyzed enantioselective synthesis of pyrazolidines, isoxazolidines, and tetrahydrooxazines. Angew Chem Int Ed. 2010; 49: 598–601.
24. Mukherjee S, List B. Chiral counteranions in asymmetric transition-metal catalysis: highly enantioselective Pd/Brønsted acid-catalyzed direct α-allylation of aldehydes. J Am Chem Soc. 2007; 129: 11336–11337. [PubMed: 17715928]
25. Li C, Wang C, Villa-Marcos B, Xiao J. Chiral counteranion-aided asymmetric hydrogenation of acyclic imines. J Am Chem Soc. 2008; 130: 14450–14451. [PubMed: 18839940]

26. Hennecke U, Müller CH, Fröhlich R. Enantioselective haloetherification by asymmetric opening of*meso*-halonium ions. Org Lett. 2011; 13: 860–863. [PubMed: 21302896]
27. Liao S, List B. Asymmetric counteranion-directed transition-metal catalysis: enantioselective epoxidation of alkenes with manganese (III) salen phosphate complexes. Angew Chem Int Ed. 2010; 49: 628–631.
28. Merten C, Pollok CH, Liao S, List B. Stereochemical communication within a chiral ion pair catalyst. Angew Chem Int Ed. 2015; 54: 8841–8845.
29. Rutten MGTA, Vaandrager FW, Elemans JAAW, Nolte RJM. Encoding information into polymers. Nat Rev Chem. 2018; 2: 365–381.
30. Pizzolato SF, Štacko P, Kistemaker JC, van Leeuwen T, Feringa BL. Phosphoramidite-based photoresponsive ligands displaying multifold transfer of chirality in dynamic enantioselective metal catalysis. Nat Catal. 2020; 3: 488–496.
31. Feringa BL. The art of building small: from molecular switches to motors (Nobel lecture). Angew Chem Int Ed. 2017; 56: 11060–11078.
32. Kistemaker JC, Pizzolato SF, van Leeuwen T, Pijper TC, Feringa BL. Spectroscopic and theoretical identification of two thermal isomerization pathways for bistable chiral overcrowded alkenes. Chem Eur J. 2016; 22: 13478–13487. [PubMed: 27471009]
33. Zhang W, Loebach JL, Wilson SR, Jacobsen EN. Enantioselective epoxidation of unfunctionalized olefins catalyzed by salen manganese complexes. J Am Chem Soc. 1990; 112: 2801–2803.
34. Irie R, Noda K, Ito Y, Matsumoto N, Katsuki T. Catalytic asymmetric epoxidation of unfunctionalized olefins. Tetrahedron Lett. 1990; 31: 7345–7348.
35. Liao S, List B. Asymmetric counteranion-directed iron catalysis: a highly enantioselective sulfoxidation. Adv Synth Catal. 2012; 354: 2363–2367.
36. McGarrigle EM, Gilheany DG. Chromium-and manganese-salen promoted epoxidation of alkenes. Chem Rev. 2005; 105: 1563–1602. [PubMed: 15884784]
37. Vicario J, Walko M, Meetsma A, Feringa BL. Fine tuning of the rotary motion by structural modification in light-driven unidirectional molecular motors. J Am Chem Soc. 2006; 128: 5127–5135. [PubMed: 16608348]
38. Štacko P, et al. Locked synchronous rotor motion in a molecular motor. Science. 2017; 356: 964–968. [PubMed: 28572394]
39. Skarżewski J, Gupta A, Vogt A. Influence of additional ligands on the two-phase epoxidation with sodium hypochlorite catalysed by (salen)manganese(III) complexes. J Mol Catal Chem. 1995; 103: L63–L68.
40. Jacobsen EN, Zhang W, Muci AR, Ecker JR, Deng L. Highly enantioselective epoxidation catalysts derived from 1,2-diaminocyclohexane. J Am Chem Soc. 1991; 113: 7063–7064.

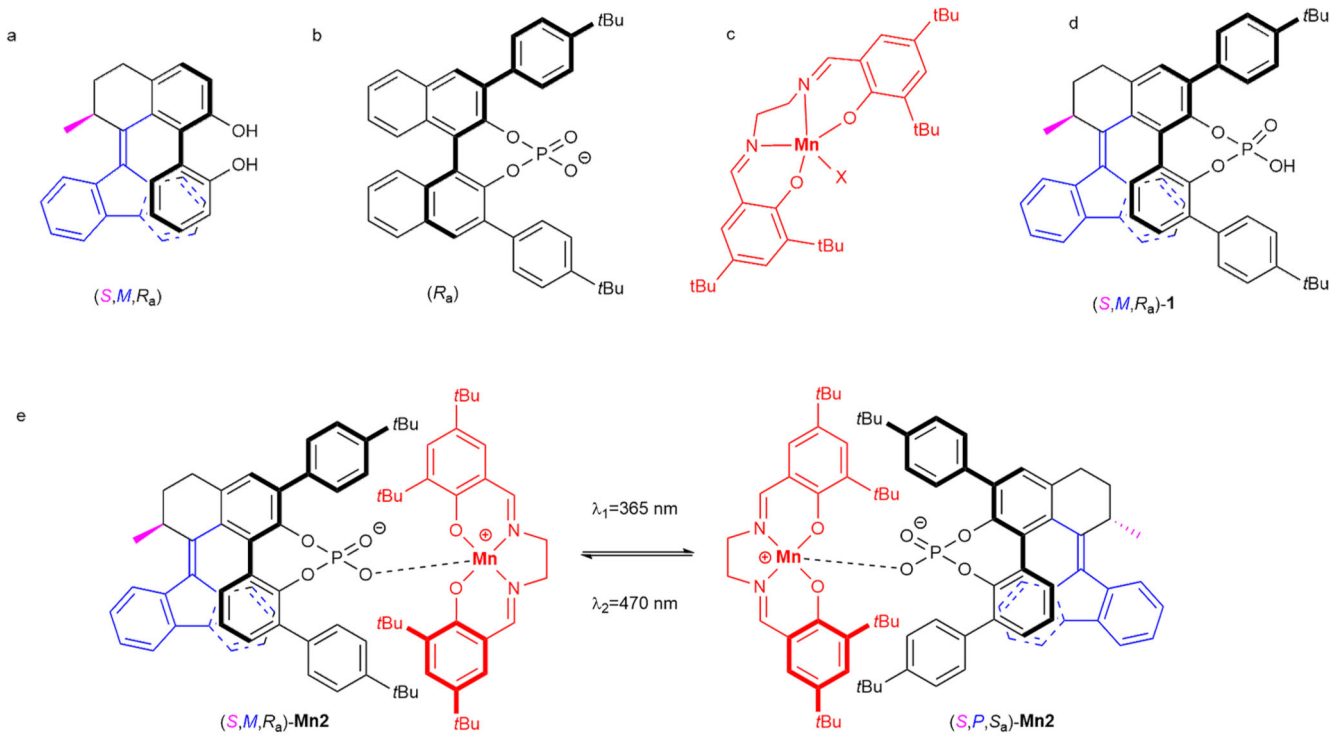

Fig. 1. Structures of compounds.

a Structure of a light-responsive 2,2'-biphenol-derived ligand based on a second-generation molecular motor.[10] **b** Structure of a bulky BINOL-derived phosphate anion (BINOL stands for 1,1'-bi-2-naphthol). **c** Structure of a manganese (III) salen complex. **d** Structure of the molecular motor-based phosphoric acid. **e** Light-induced switching between the pseudo-enantiomers of the ion-paired complexes (*S, M,R*$_a$)-**Mn2** and (*S,P,S*$_a$)-**Mn2**. The bold bonds represent the parts of the molecules that are closer to the viewer, to help represent the dimensionality of the structures.

Europe PMC Funders Author Manuscripts

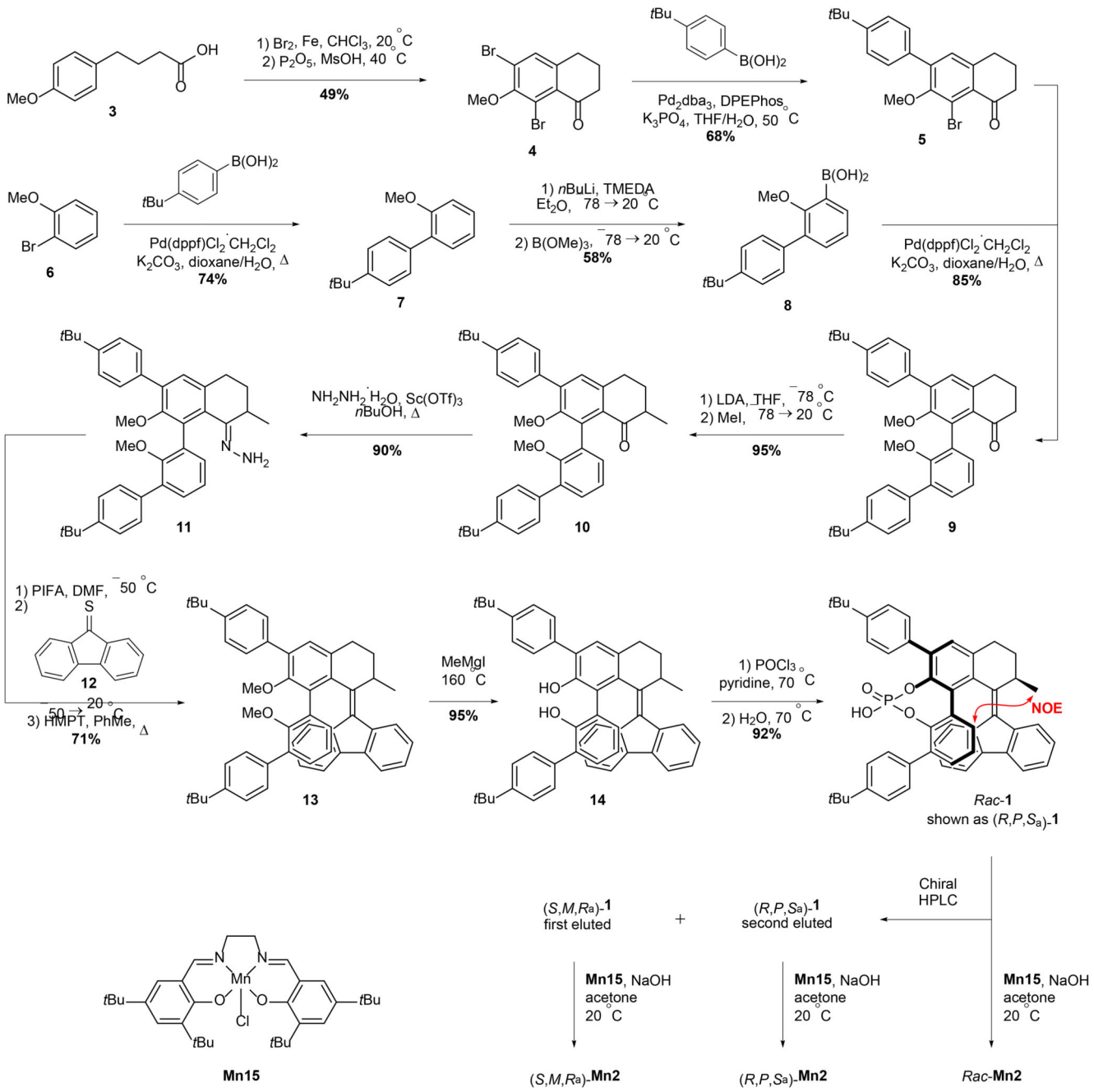

Fig. 2. Synthesis and resolution of ion-paired switch-manganese(III) salen catalyst Mn2.

Conformationally flexible compounds **10**, **11**, **13**, and **14** were obtained as racemic mixtures, and each enantiomer was composed of a mixture of two axially chiral conformers, see Supplementary section 1.2 for further details. The red arrow in structure *Rac*-**1** denotes the NOE-effect that was used to confirm the relative stereochemistry of this compound. The bold bonds in *Rac*-**1** represent the parts of the molecule that are closer to the viewer, to help represent the dimensionality of the structure. Abbreviations: Ms, methanesulfonyl; dba, dibenzylideneacetone;

Europe PMC Funders Author Manuscripts

DPEPhos, bis[(2-diphenylphosphino)phenyl] ether; THF, tetrahydrofuran; dppf, 1,1’-bis(diphenylphosphino)ferrocene; TMEDA, tetramethylethylenediamine; LDA, lithium diisopropylamide; PIFA, [bis(trifluoroacetoxy)]iodobenzene; DMF, dimethylformamide; HMPT, tris(dimethylamino)phosphine; NOE, nuclear Overhauser effect; HPLC, high-performance liquid chromatography.

Europe PMC Funders Author Manuscripts

Europe PMC Funders Author Manuscripts

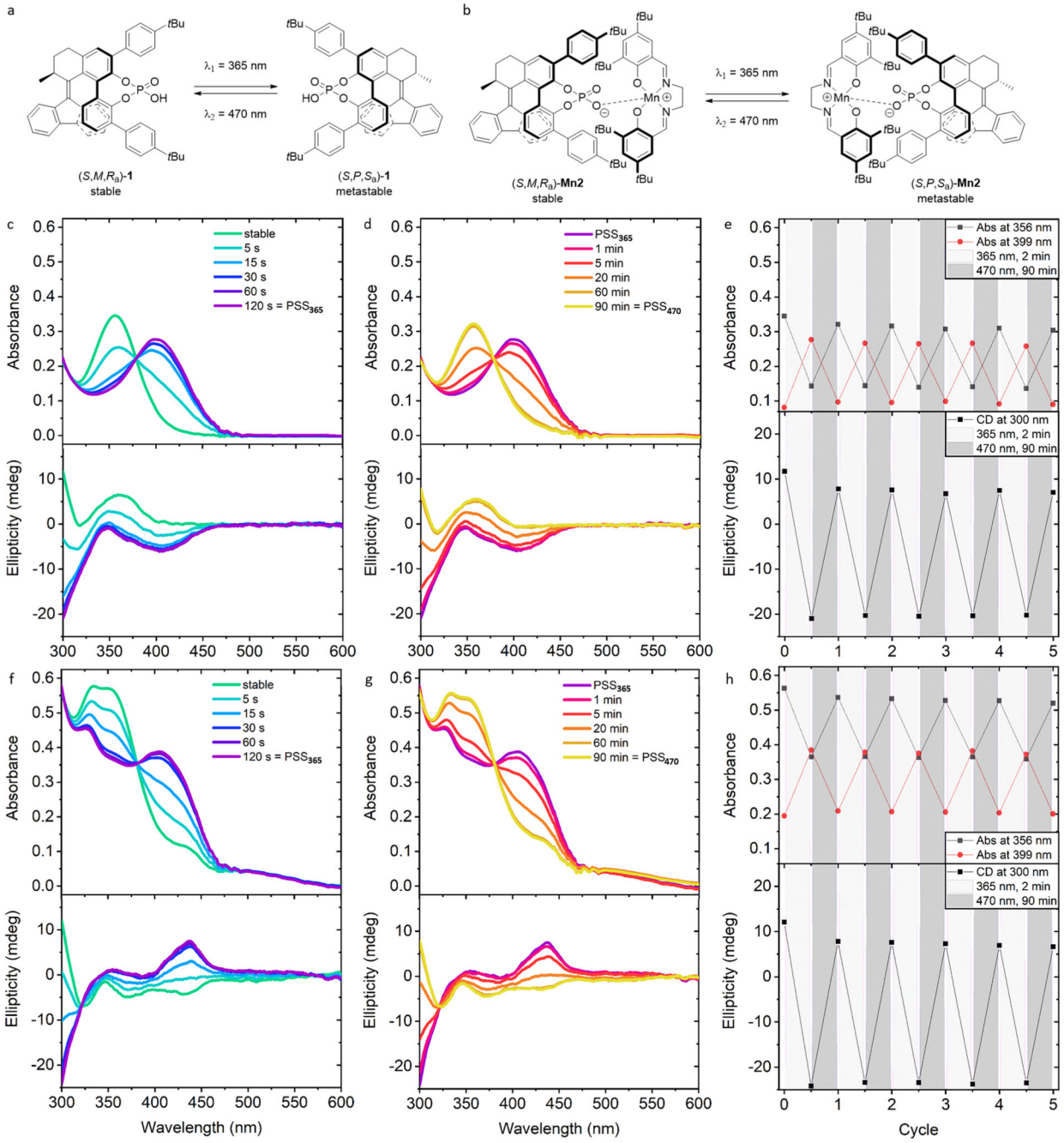

Fig. 3. UV-vis and CD spectroscopic studies of the photochemical switching of (*S,M,R*$_a$)-1 and (*S,M,R*$_a$)-Mn2.

a Scheme showing the reversible switching of **1**. **b** Scheme showing the reversible switching of **Mn2**. **c** UV-vis (top) and CD (bottom) spectra of (*S,M,R*$_a$)-**1** during irradiation with UV light (λ = 365 nm). **d** UV-vis (top) and CD (bottom) spectra of (*S,M,R*$_a$)-***1*** during switching from the metastable to the stable state upon irradiation with visible light (λ = 470 nm). **e** Irradiation cycles of (*S,M,R*$_a$)-**1** monitored with UV-vis (top) and CD spectroscopy (bottom). **f** UV-vis (top) and CD (bottom) spectra of (*S,M,R*$_a$)-**Mn2** during

switching from the stable to the metastable state upon irradiation with UV light (λ = 365 nm); **g** UV-vis (top) and CD (bottom) spectra of (*S*,*M*,*R*$_a$)-**Mn2** during switching from the metastable to the stable state upon irradiation with visible light (λ = 470 nm). **h** Irradiation cycles of (*S*,*M*,*R*$_a$)-**Mn2** monitored with UV-vis (top) and CD spectroscopy (bottom). For all experiments concentration = 10^{-4} M in benzene, *l* = 2 mm. The bold bonds in **a** and **b** represent the parts of the molecules that are closer to the viewer, to help represent the dimensionality of the structures. Abbreviations: CD, circular dichroism; PSS, photostationary state; Abs, absorption.

Europe PMC Funders Author Manuscripts

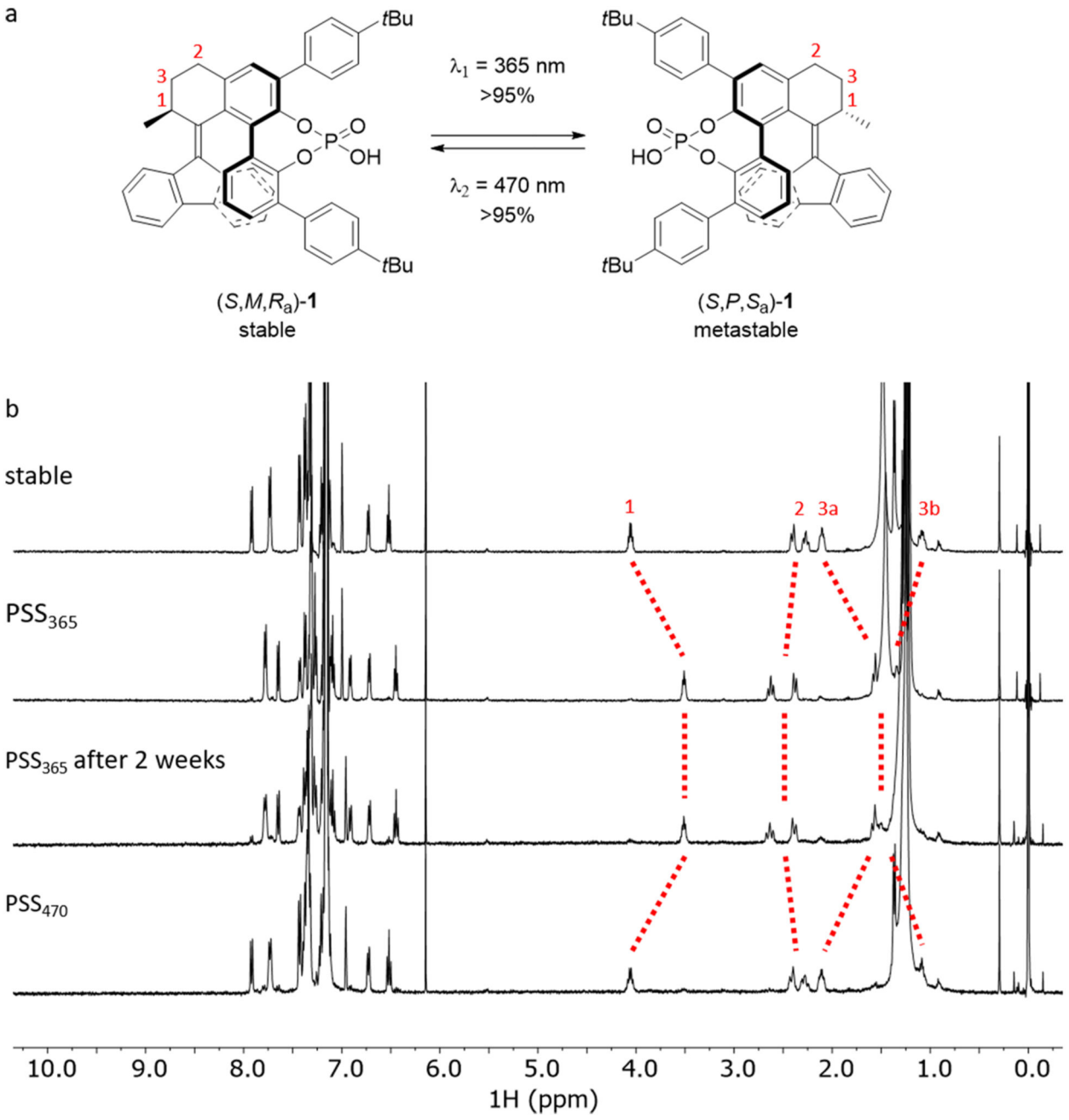

Fig. 4. NMR spectroscopy study of the photochemical switching of *Rac*-1.

a Schematic representation of the reversible switching of **1**; for clarity, only one of the enantiomers (*S,M,R*$_a$) is shown. **b** ^{1}H NMR spectra of *Rac*-**1** (C_6D_6, 298 K, concentration = 2×10^{-3} M); from top to bottom: stable *Rac*-**1** state before irradiation (stable); stable *Rac*-**1** after irradiation to the metastable state with UV light at λ = 365 nm for 45 min (PSS_{365}); metastable *Rac*-**1** after leaving the PSS_{365} mixture standing for 2 weeks (PSS_{365} after 2 weeks); metastable *Rac*-**1** after irradiation of the PSS_{365}-mixture with visible light at λ = 470 nm for 18 h, resulting in almost complete isomerization of *Rac*-**1** back to its stable state

(PSS_{470}). The atoms labelled as 1, 2 and 3 in Fig. 4a are compared in the spectra in Fig 4b. The bold bonds in Fig 4a represent parts of the molecules that are closer to the viewer to help represent the dimensionality of the structures. Abbreviation: PSS, photostationary state.

Europe PMC Funders Author Manuscripts

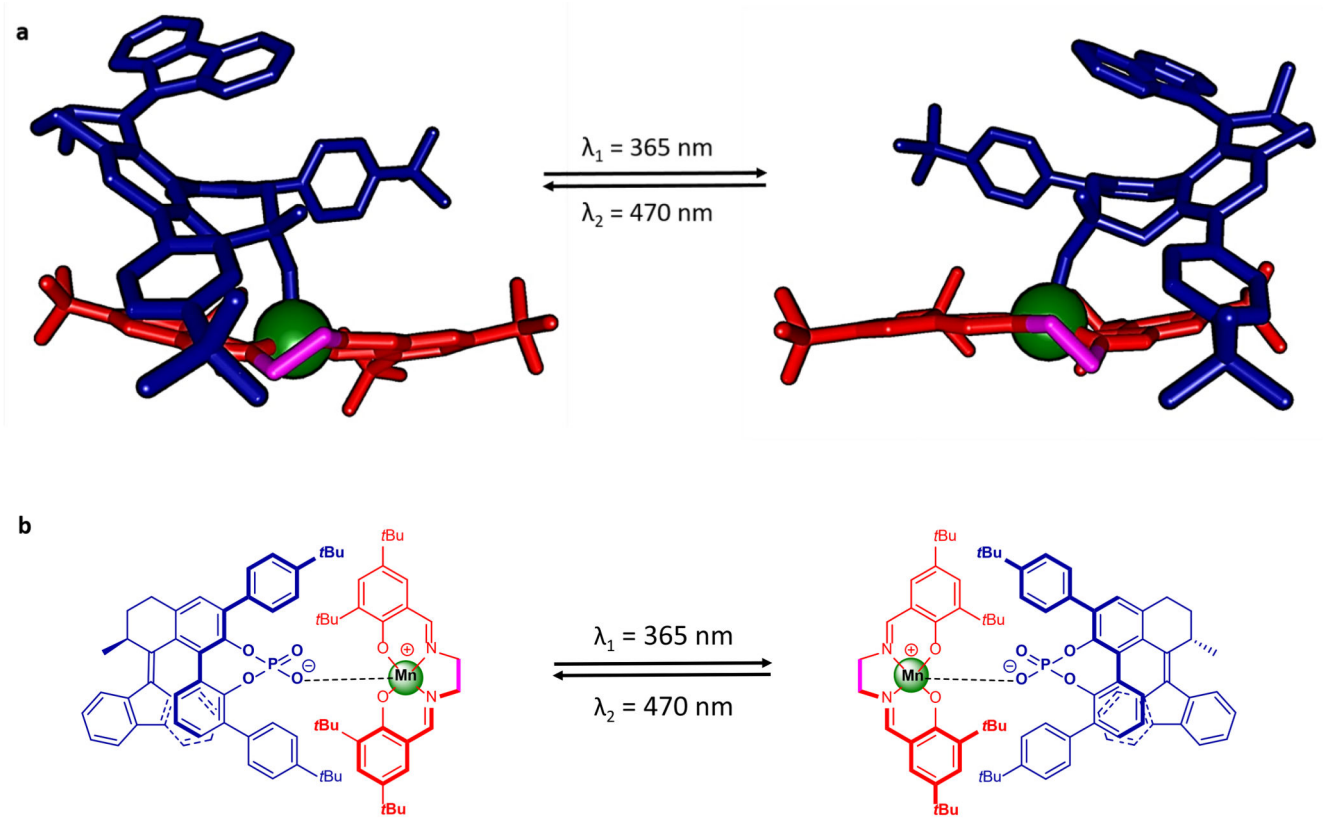

Fig. 5. X-ray crystal structures of the stable and metastable forms of Mn2.

a, **left** Front view of the X-ray structure of the stable (*S*,*M*,R_a)-**Mn2** isomer; **a**, **right** Front view of the X-ray structure of the metastable (*S*,*P*,S_a)-**Mn2** isomer. For ease of comparison in the same color coding: **b**, **left** schematic structure of (*S*,*M*,R_a)-**Mn2** and **b**, **right** schematic structure of (*S*,*P*,S_a)-**Mn2**. Color coding: blue is phosphate ligand **1**; red is salen ligand; magenta is ethylene bridge of salen ligand; green is manganese center; hydrogen atoms have been omitted for clarity. The single crystal structures shown in **5a** were selected from the crystal structures of stable *Rac*-**Mn2** and metastable *Rac*-**Mn2**, respectively (for more detailed crystal data see Supplementary section 4). The bold bonds represent parts of the molecules that are closer to the viewer, to help represent the dimensionality of the structures.

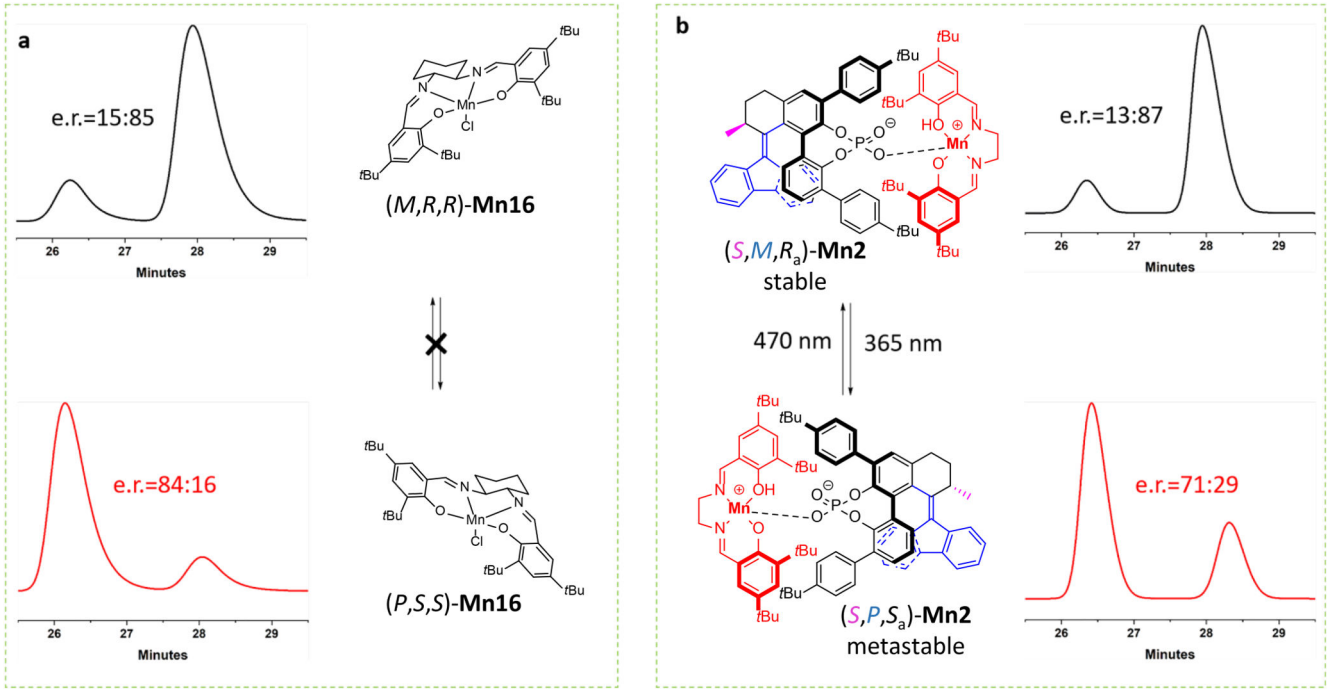

Fig. 6. Enantioselective epoxidations.

Enantioselective epoxidation of **17** and determination of the absolute configuration of the catalysts, based on the chiral HPLC traces of the product mixture of the epoxidation catalyzed by **a** (top) (*M*,*R*,*R*)-**Mn16**, **b** (top) (*S*,*M*,R_a)-**Mn2**, **a** (bottom) (*P*,*S*,*S*)-**Mn16** and **b** (bottom) (*S*,*P*,S_a)-**Mn2**. The bold bonds represent parts of the molecules that are closer to the viewer to help represent the dimensionality of the structures. Abbreviation: e.r., enantiomeric ratio.

Europe PMC Funders Author Manuscripts

Table 1

Enantiodivergent epoxidation of alkenes using Mn2 as the catalyst.[a]

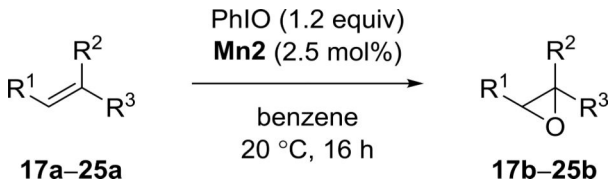

Entry	Substrate	Product	Catalyst	Conv. (%)[b]	Yield (%)[c]	e.e. (%)[d]	Δe.e.(%)	e.d.(%)[e]
1[f]	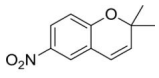 17a	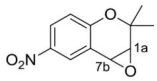 17b	(*S*,*M*,R_a)-**Mn2**	97–99	86–90	70–74	112–118	57–63
2[g]			(*S*,*P*,S_a)-**Mn2**	90–93	73–79	(1a*R*,7b*R*) 42–44 (1a*S*,7b*S*)		
3[f]			(*R*,*P*,S_a)-**Mn2**	92–95	75–79	68–70(1a*S*,7b*S*)	110–114	60–65
4[h]			(*R*,*M*,R_a)-**Mn2**	95–96	82–85	42–44(1a*R*,7b*R*)		
5	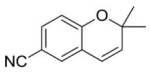 18a	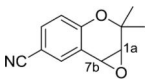 18b	(*S*,*M*,R_a)-**Mn2**	95–98	85–90	74–78(1a*R*,7b*R*)	90–98	21–27
6[g]			(*S*,*P*,S_a)-**Mn2**	90–92	74–76	16–20(1a*S*,7b*S*)		
7	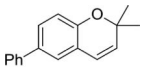 19a	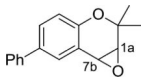 19b	(*S*,*M*,R_a)-**Mn2**	89–90	75–80	52–56 (1a*R*,7b*R*)	92–98	71–81
8[g]			(*S*,*P*,S_a)-**Mn2**	82–85	62–67	40–42 (1a*S*,7b*S*)		
9	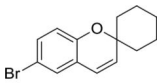 20a	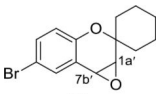 20b	(*S*,*M*,R_a)-**Mn2**	95–96	81–85	50–52 (1a′ *R*,7b′ *R*)	80–84	58–64
10[g]			(*S*,*P*,S_a)-**Mn2**	95–98	83–85	30–32 (1a′ *S*,7b′ *S*)		
11	 21a	 21b	(*S*,*M*,R_a)-**Mn2**	85–90	63–66	22–24 (*R*)	34–40	50–73
12[g]			(*S*,*P*,S_a)-**Mn2**	74–78	53–62	12–l6 (*S*)		
13	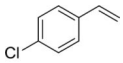 22a	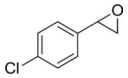 22b	(*S*,*M*,R_a)-**Mn2**	90–96	83–88	12–16 (*R*)	22–28	62–100
14[g]			(*S*,*P*,S_a)-**Mn2**	95–98	83–85	10–12(*S*)		
15	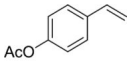 23a	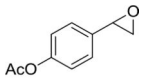 23b	(*S*,*M*,R_a)-**Mn2**	96–97	89–91	16–20 (*R*)	26–36	50–100
16[g]			(*S*,*P*,S_a)-**Mn2**	96–97	85–88	10–16 (*S*)		
17	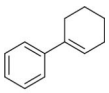 24a	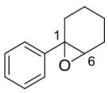 24b	(*S*,*M*,R_a)-**Mn2**	72–76	60–68	12–14 (1*S*,6*S*)	18–26	43–100
18[g]			(*S*,*P*,S_a)-**Mn2**	68–70	50–51	6–12 (1*R*,6*R*)		
19	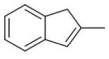 25a	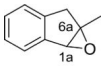 25b	(*S*,*M*,R_a)-**Mn2**	59–68	27–35	22–30 (1a*R*,6a*S*)	32–42	33–55
20[g]			(*S*,*P*,S_a)-**Mn2**	51–60	30–39	10–12 (1a*S*,6a*R*)		

[a] All experiments were performed in duplicate, unless stated otherwise.

[b] Conversion was calculated based on the recovered substrate.

[c] Isolated yield.

[d] Enantiomeric excess (e.e.) values were determined by chiral HPLC. See the Supplementary Information for the assignment of the absolute configurations of the enantioenriched epoxides.

[e] Enantio-divergence (e.d.) is defined as the ratio of the e.e. values of the enantioenriched epoxides when produced by metastable-**Mn2** versus stable-**Mn2**.

[f] Experiment was performed in triplicate.

[g] Catalyst (*S,P,S*$_a$)-**Mn2** was obtained by irradiation of (*S,M,R*$_a$)-**Mn2** (concentration = 1 mg/mL in CH_2Cl_2) for 30 min with λ = 365 nm light, followed by evaporation of the solvent.

[h] Catalyst (*R,M,R*$_a$)-**Mn2** was obtained by irradiation of (*R,P,S*$_a$)-**Mn2** (concentration = 1 mg/mL in CH_2Cl_2) for 30 min with λ = 365 nm light, followed by evaporation of the solvent. Abbreviations: OAc, acetyloxy; Ph, phenyl.

Europe PMC Funders Author Manuscripts